

Modulation of Circulating Angiogenic Factors and Tumor Biology by Aerobic Training in Breast Cancer Patients Receiving Neoadjuvant Chemotherapy

Lee W. Jones¹, Diane R. Fels¹, Miranda West¹, Jason D. Allen¹, Gloria Broadwater¹, William T. Barry¹, Lee G. Wilke², Elisabeth Masko¹, Pamela S. Douglas¹, Rajesh C. Dash¹, Thomas J. Povsic¹, Jeffrey Peppercorn¹, P. Kelly Marcom¹, Kimberly L. Blackwell¹, Gretchen Kimmick¹, Timothy G. Turkington¹, and Mark W. Dewhirst¹

Abstract

Aerobic exercise training (AET) is an effective adjunct therapy to attenuate the adverse side-effects of adjuvant chemotherapy in women with early breast cancer. Whether AET interacts with the antitumor efficacy of chemotherapy has received scant attention. We carried out a pilot study to explore the effects of AET in combination with neoadjuvant doxorubicin–cyclophosphamide (AC+AET), relative to AC alone, on: (i) host physiology [exercise capacity (VO_2 peak), brachial artery flow-mediated dilation (BA-FMD)], (ii) host-related circulating factors [circulating endothelial progenitor cells (CEP) cytokines and angiogenic factors (CAF)], and (iii) tumor phenotype [tumor blood flow (^{15}O -water PET), tissue markers (hypoxia and proliferation), and gene expression] in 20 women with operable breast cancer. AET consisted of three supervised cycle ergometry sessions/week at 60% to 100% of VO_2 peak, 30 to 45 min/session, for 12 weeks. There was significant time \times group interactions for VO_2 peak and BA-FMD, favoring the AC+AET group ($P < 0.001$ and $P = 0.07$, respectively). These changes were accompanied by significant time \times group interactions in CEPs and select CAFs [placenta growth factor, interleukin (IL)-1 β , and IL-2], also favoring the AC+AET group ($P < 0.05$). ^{15}O -water positron emission tomography (PET) imaging revealed a 38% decrease in tumor blood flow in the AC+AET group. There were no differences in any tumor tissue markers ($P > 0.05$). Whole-genome microarray tumor analysis revealed significant differential modulation of 57 pathways ($P < 0.01$), including many that converge on NF- κ B. Data from this exploratory study provide initial evidence that AET can modulate several host- and tumor-related pathways during standard chemotherapy. The biologic and clinical implications remain to be determined. *Cancer Prev Res*; 6(9); 925–37. ©2013 AACR.

Introduction

Randomized trials provide promising evidence that supervised aerobic exercise training (AET) is an effective adjunct strategy to prevent and/or attenuate chemotherapy-associated toxicity in patients with early-stage cancer (1, 2). Specifically, in the setting of early breast cancer, AET during concurrent adjuvant chemotherapy is associated with favorable improvements in measures of exercise capacity, functional quality-of-life, and other selected patient-reported outcomes (PRO), with few adverse events (3–5). On the basis of the current evidence base, several international agencies have published cancer-specific exercise guidelines for patients with cancer both during and following the

completion of primary therapy (4–8). Although the importance of AET to improve symptom-control outcomes in patients receiving cytotoxic therapy is undisputed, a critical corollary to this line of investigation is whether AET interacts with the anticancer efficacy of chemotherapy (9).

Such an interaction is biologically plausible as AET is a pleiotropic therapy shown to modulate a wide spectrum of host (systemic)-related pathways including immune/inflammation, metabolism, and steroid sex hormones (10). Modulation of one or more of these pathways could alter growth factor/ligand availability in peripheral blood as well as in the tumor microenvironment that, via paracrine or autocrine signaling, could alter tumor cell signal transduction and phenotype and potentially, response to anti-cancer therapy (11). For example, breast tumors have an abnormal vascular system that impairs effective oxygen and drug transport (12, 13). The resultant hypoxia is associated with drug resistance (12, 14) and greater likelihood for metastasis (15, 16). To this end, it is well-established that AET exerts multiple favorable provascular/angiogenic effects both in the systemic host vasculature as well as regionally in heart and skeletal muscle in patients with

Authors' Affiliations: ¹Duke University Medical Center, Durham, North Carolina; and ²Division of General Surgery, University of Wisconsin, Madison, Wisconsin

Corresponding Author: Lee W. Jones, Duke Cancer Institute, Duke University Medical Center, Box 3085, Durham, NC 27710. Phone: 919-668-6791; Fax: 919-681-1282; E-mail: lee.w.jones@duke.edu

doi: 10.1158/1940-6207.CAPR-12-0416

©2013 American Association for Cancer Research.

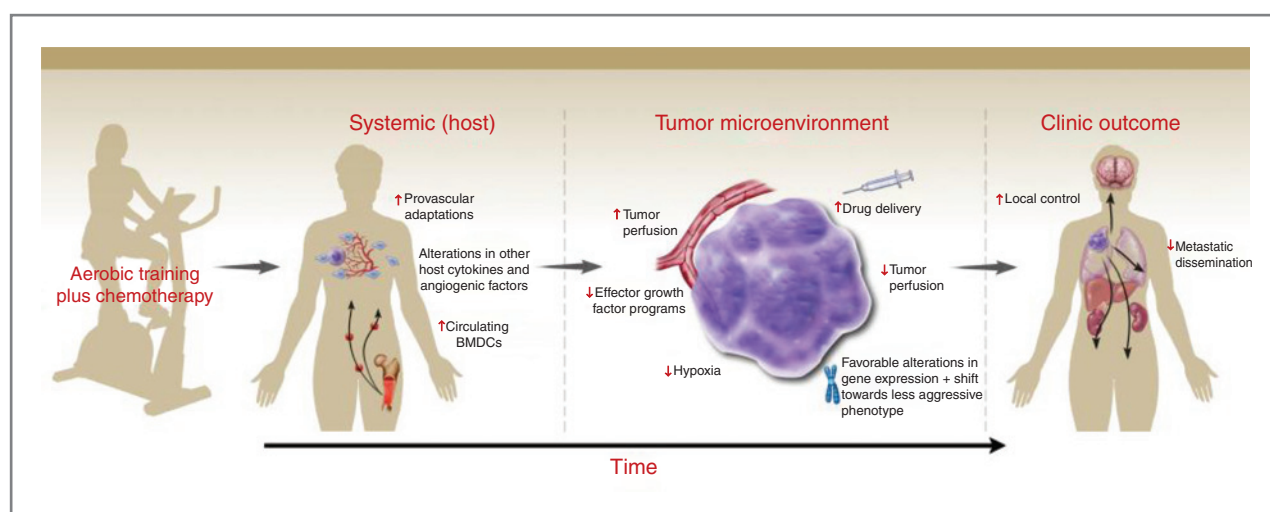


Figure 1. Conceptual model. Schematic representation of the postulated multistep process of AET-induced upregulation of systemic host factors (e.g., NO bioavailability, CEPs) alter the tumor microenvironment leading to an acute increase in tumor perfusion (vascularization) which, when combined with chemotherapy, may lead to improved drug delivery with the net effect of reduced tumor perfusion (enhanced tumor cell kill) with accompanying favorable alterations in tumor gene expression with a shift toward a less aggressive phenotype.

ischemic disease such as peripheral artery disease, myocardial infarction, and heart failure (17–22).

AET-induced favorable vascular adaptations are mediated, in part, via increased bioavailability of nitric oxide (NO), a potent regulator of peripheral vasomotor-regulated blood flow (23–25). Interestingly, NO also activates the release and mobilization of circulating endothelial progenitor cells (CEP; ref. 26). In the context of ischemic cardiovascular disease, mobilized CEPs enhance angiogenesis and vascular repair, improve endothelial function, and recovery of the myocardium after ischemia and infarction (27–34). However, in the setting of hypoxic solid tumors, CEPs have been shown to be home to primary solid tumors contributing to angiogenesis (neovascularization) and potentially tumor cell repopulation/regrowth in between chemotherapy cycles (35, 36). Intriguingly, chronic AET increases the production, mobilization, and number of circulating CEPs in noncancer clinical populations (22, 37, 38).

Given the established provascular/angiogenic effects of AET together with the critical importance of tumor hypoxia in cancer progression and therapeutic response, our group has carried out several preclinical studies to investigate the effect of AET on tumor hypoxia/physiology in clinically relevant mouse models. Intriguingly, we found that while primary tumor growth rate was comparable between exercise and control groups, similar to the provascular effects of AET in models of cardiac and hindlimb ischemia, tumors from exercised mice had significantly increased intratumoral perfusion/vascularization (or physiologic angiogenesis) in orthotopic models of breast and prostate cancer (11, 39). Overall, our initial observations indicate that AET promotes a shift toward a more "normalized" tumor microenvironment. Thus, given that hypoxia is a major obstacle to the delivery and efficacy of chemotherapy, the combination of chemotherapy and

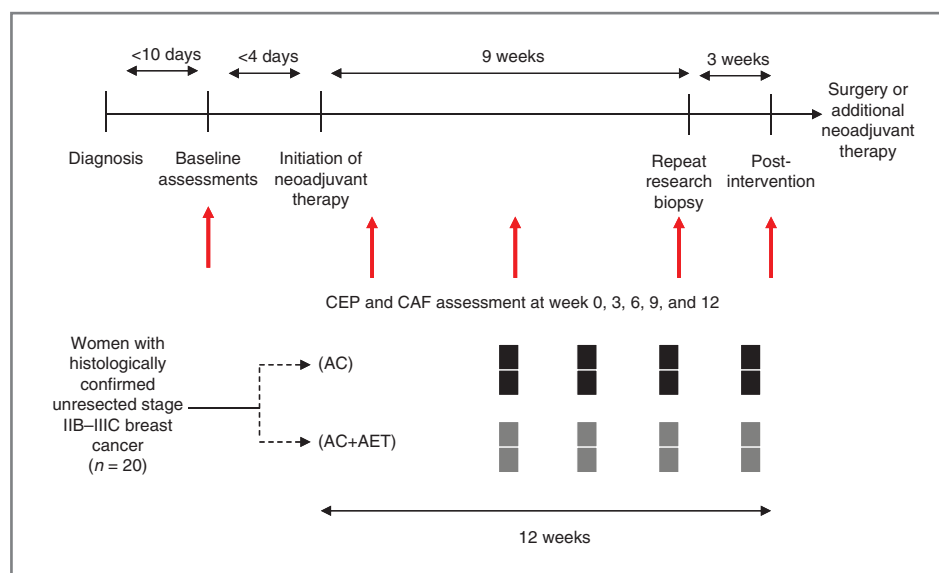
AET could be an effective strategy to improve chemosensitivity in solid tumors (Fig. 1).

As a first step toward more definitive clinical studies, the purpose of this study was to explore the effects of AET on several relevant host-related factors that could potentially modulate the antitumor properties of chemotherapy. We also explore whether modulation of host-related factors altered tumor tissue markers. To address this question, we carried out a phase II study to investigate the effects of AET in combination with neoadjuvant chemotherapy [doxorubicin–cyclophosphamide (AC+AET)], relative to AC alone, on: (i) host physiology/cardiovascular function (exercise capacity and peripheral vascular endothelial function), (ii) host-related circulating (systemic) factors [CEPs and other proinflammatory cytokines and angiogenic factors (CAF)], (iii) tumor phenotype (proliferation and apoptosis) and physiology [microvessel density (MVD), hypoxia, and tumor blood flow]; and (iv) tumor gene expression.

Materials and Methods

Full details about the study sample, recruitment, and procedures have been reported elsewhere (40). In brief, 20 women with newly diagnosed, histologically confirmed unresected stage IIB–IIIC breast adenocarcinoma scheduled for first-line neoadjuvant chemotherapy at Duke Cancer Institute (DCI; Durham, NC) were studied. Other major eligibility criteria were: (i) Karnofsky performance status >70, (ii) no previous history of malignancy, (iii) absence of significant cardiac disease, (iv) absence of contraindications to neoadjuvant chemotherapy, (v) no absolute contraindications to supervised aerobic training based on a CPET, (vi) willingness to travel to DCI to attend supervised aerobic training sessions three times a week, and (vii) primary attending oncologist approval (determination of eligibility

Figure 2. Trial design schema and timing of study endpoints.



was at the discretion of the attending oncologist). The distinct advantage of the neoadjuvant setting is that it permits assessment of tumor-related outcomes, in conjunction with plasma and imaging correlative science biomarkers, that is not possible in the adjuvant (postsurgery) setting.

Following successful completion of all baseline assessments, participants were randomly allocated to ($n = 10/\text{group}$): (i) four cycles of neoadjuvant doxorubicin ($60 \text{ mg}/\text{m}^2$) in combination with cyclophosphamide ($600 \text{ mg}/\text{m}^2$; AC) every 3 weeks (i.e., 12 weeks in duration) or (ii) AC+AET (Fig. 2). All study procedures were reviewed and approved by the Duke University Medical Center (DUMC; Durham, NC) Institutional Review Board. All subjects signed a written consent before the initiation of any study-related procedures. Trial registration number is NCT00405678.

Supervised aerobic exercise training

The AET intervention was developed using a nonlinear periodized approach applying the principles of training, permitting the design of patient-specific individualized exercise prescriptions. In terms of the general exercise prescription, AET consisted of three (frequency) supervised aerobic cycle ergometry (modality) sessions per week, 20 to 45 min/session (duration), at 55% to 100% of $\text{VO}_{2 \text{ peak}}$ (intensity), on nonconsecutive days for 12 weeks (length). AET intensity was based on the workload (W) corresponding to a specific percentage of $\text{VO}_{2 \text{ peak}}$ (e.g., 55% and 65%) elicited during the prerandomization CPET and was designed to improve $\text{VO}_{2 \text{ peak}}$ (Fig. 3). AET sessions were sequenced in such a fashion that exercise-induced physiologic stress is continually altered in terms of intensity and duration in conjunction with appropriate rest and recovery sessions to optimize adaptation in the outcome of interest. AET intensity and safety was monitored continuously via heart rate and oxyhemoglobin saturation (SpO_2), whereas

blood pressure was monitored at the beginning, middle, and end of each session. Participants randomized to neoadjuvant chemotherapy (usual care) were instructed to maintain their usual exercise levels and not to initiate a structured AET program during the study period.

Study endpoint assessments and timing

Exercise capacity, endothelial function, and tumor blood flow assessments were determined at baseline (before initiation of chemotherapy) and postintervention, after an 8-hour, water only fast at both time points, and a minimum of 48 hours following the completion of the last chemotherapy and aerobic training session (AC+AET group only) at the postintervention time point. The follow-up tumor blood flow assessment was conducted at week 9 (i.e., third cycle of AC). Serial blood collection was conducted at five time points during the study in both groups (i.e., baseline, 3, 6, 9, and 12 weeks). Blood collection was standardized across all patients in terms of day of collection and before chemotherapy administration in all patients. Two separate 8 mL EDTA blood samples were obtained. For CEP enumeration, samples were sent to a single laboratory at DUMC for traditional fluorescence activated cell sorting (FACS) analysis within 12 hours of blood extraction, as previously described (41). The other EDTA sample was processed within 12 hours for storage in a -85°C freezer. Analysis of all plasma cytokine and angiogenic factors was conducted in one batch. Tumor biopsy samples were obtained at week 9 (i.e., third cycle of AC) in both groups.

Exercise capacity

Exercise capacity was assessed using a symptom-limited CPET on an electronically braked cycle ergometer (Ergoline, Ergoselect 100) with expired gas analysis (ParvoMedics TrueOne 2400) to determine $\text{VO}_{2 \text{ peak}}$, as described previously (42). In brief, preceding exercise, 3 minutes of resting metabolic data were collected before participants began

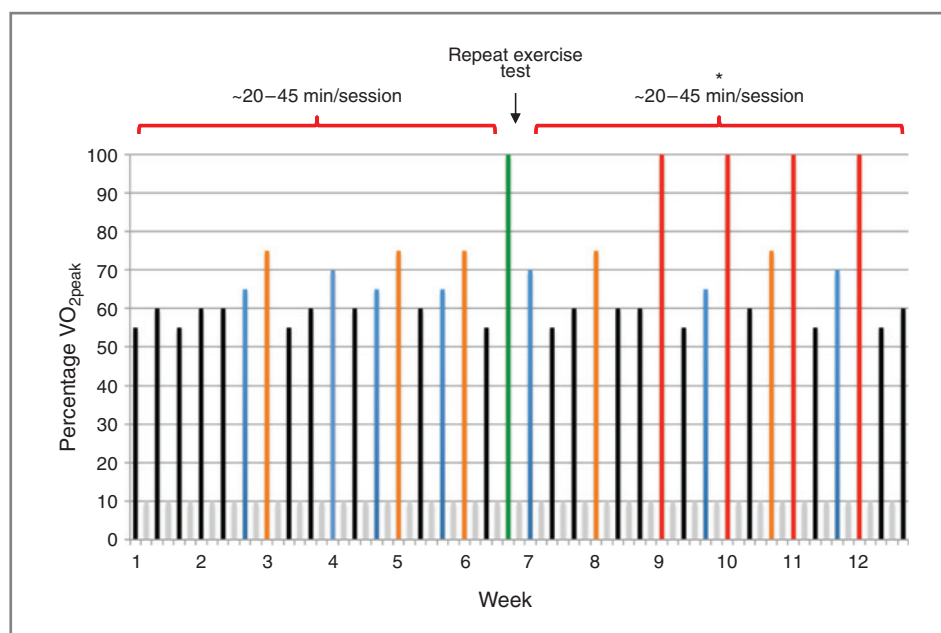


Figure 3. Exercise training intervention. Supervised AET consisted of three (frequency) supervised aerobic cycle ergometry (modality) sessions per week, 20 to 45 min/session (duration), at 55% to 100% of $VO_{2\text{ peak}}$ (intensity), on nonconsecutive days for 12 weeks (length). AET intensity was based on the workload (W) corresponding to a specific percentage of $VO_{2\text{ peak}}$ (e.g., 55% and 65%) elicited during the prerandomization CPET and was designed to improve $VO_{2\text{ peak}}$. Specifically, intensity is depicted by the colored bars as a percentage of $VO_{2\text{ peak}}$: (i) black, 55% to 60%, (ii) blue, 65% to 70%, (3) orange, 70% to 80%, (iv) red, 100%. Gray colored bars represent rest (off) days. In weeks 1 to 4, black and blue exercise sessions were approximately 20 to 30 minutes in duration; in weeks 5 to 8, black and blue sessions were approximately 30 to 45 minutes in duration, whereas orange sessions were approximately 20 to 25 minutes in duration. At the end of week 6, the CPET is repeated to rescribe AET intensity (green colored bar). Represcription of AET based on the repeat CPET is to ensure sufficient stimulus to induce further physiologic (cardiovascular) adaptation. Such an approach can also be used to rescribe AET intensity in the scenario in which patient's may have missed sessions due to illness or treatment toxicity. In weeks 9 to 12, black and blue sessions were approximately 30 to 45 minutes in duration, orange sessions were 25 minutes or more, whereas red sessions consisted of interval sessions for 30 seconds at 100% $VO_{2\text{ peak}}$ followed by 60 seconds of active recovery at approximately 50% $VO_{2\text{ peak}}$ for 10 to 20 intervals. *, Intensity of all sessions in weeks 7 to 12 are prescribed on the basis of the results of the repeat CPET at the end of week 6.

cycling at 20 W. Workloads were then increased 5 to 20 W/min until volitional exhaustion or symptom-limitation. Workload increments were determined by patient cardiopulmonary response to exercise during the first minute of exercise and were standardized at baseline and postintervention. All CPET data were recorded as the highest 30-second value elicited during the exercise test. During exercise, heart rate and rhythm and SpO_2 were monitored continuously using a 12-lead electrocardiography (ECG) and pulse oximetry (BCI; Hand-Held Pulse Oximeter). No serious adverse events were observed during CPET procedures (40).

Brachial artery flow-mediated dilation (endothelial function)

Vascular endothelial function was measured by brachial artery flow-mediated dilation (BA-FMD). All vascular imaging was carried out with the participant in a supine position with the forearm extended and slightly supinated. BA-FMD assessments were obtained using high-resolution ultrasound and a 7.5 MHz linear array transducer (Accuson, Sequoia 512), at baseline (following 10 minute of supine rest), during 5 minutes of forearm occlusion, and continuously on r-wave trigger for 2 minutes following cuff release (hyperemia) as previously described (43). Arterial diameter

and blood flow was measured from the digital recordings. Diameters were determined from the anterior to posterior interface between the intimal layers. The percentage change in brachial artery diameter was calculated by the following formula (at rest, 60 seconds post-cuff release, and peak):

$$\left[\frac{(\text{peak post} - \text{hyperemia diastolic diameter} - \text{baseline diastolic diameter})}{\text{baseline diastolic diameter}} \right] \times 100$$

Reproducibility of the BA-FMD technique has previously yielded average mean differences in brachial artery diameter change for days, testers, and readers of 1.91%, 1.40%, and 0.21 mm, respectively, with intraclass correlation coefficients of 0.92, 0.94, and 0.90, respectively (44).

Circulating endothelial progenitor cells

Peripheral blood mononuclear cells were isolated from 7 to 10 mL of blood by differential centrifugation, as previously described (PMID: 23359346). In brief, after plasma removal, the buffy coat was transferred to a 50 mL conical tube and isolated mononuclear cells were washed with Iscove's modified Dulbecco's medium (IMDM) containing 2% fetal calf serum (IMDM+2%) concentrated in 10^7 cells/mL in 80 μ L IMDM+2%. Nonspecific antibody binding was

inhibited using FcR reagent (Becton Dickinson; 10 μ L \times 10 minutes), and cells were incubated with CD-133- allophycocyanin (Miltenyi Biotec), VEGFR-2-phycoerythrin (R&D Systems), and aldehyde dehydrogenase (ALDH) activity for 60 minutes at 4°C. These are well-established cell surface markers of bone marrow-derived CEPs (45). Dead and dying cells were excluded using 7-amino-actinomycin D (7-AAD; Invitrogen) added just before nonautomated FACS analysis.

Total human peripheral blood was analyzed for the relative content of cells with low orthogonal light scatter and high ALDH activity content [side scatter low (SSC^{lo}) ALDH-bright (ALDH^{br}) cells]. Briefly, 4 \times 10⁶ cells were aliquoted for analysis into an Aldecoum tube containing 2 mL of Aldecoum buffer (Aldagen Inc.). Immediately after addition of the cells, 500 μ L was transferred to a tube containing diethylaminobenzaldehyde, a potent inhibitor of ALDH activity (10 μ mol/L). After 30 minutes at 37°C, the cells were centrifuged, placed on ice, and flow cytometry was conducted (46). Flow cytometry was conducted using an LSR CANTO flow cytometer (BD Biosciences) and analyzed using FlowJo software (TreeStar). All cellular analyses were conducted within 2 hours of sample acquisition.

Serum cytokines and angiogenic factors

A total of 19 CAFs were assessed using multiplex ELISA-based assays conducted in triplicate on the MSD Sector Imager 2400 (Mesoscale Discovery, Inc.) using either the Human MMP 3-Plex Kit (Mesoscale #N45034A-1), Proinflammatory 9-Plex Kit (Mesoscale #N05007A-1), Bone Panel II Kit (Mesoscale #N75147A-1), or the Human Growth Factor I Kit (Mesoscale #N45029B-1) as per the manufacturer's instructions. Serial patient samples were assessed simultaneously on the same plate to minimize interassay variability.

Tumor blood flow/perfusion (¹⁵O-water PET)

Subjects were scanned on an advance positron emission tomography (PET) scanner or Discovery STE (See and Treat Elite) PET/CT (GE Healthcare Technologies). Subjects were injected with 180 \pm 9 MBq [¹⁵O] water and scanned dynamically. Images were obtained from data covering 30 to 90 seconds postinjection. Data were corrected for attenuation, scatter, and dead time random events and reconstructed with filtered back projection. Regions of interest (ROI) were placed within the breast tumors in the PET images, aided by the known tumor locations from existing imaging studies and from the computed tomography (CT) of PET/CT, when available. An index of blood flow was calculated as the average value in the tumor ROI divided by the average value in the contralateral background ROI.

Hematoxylin and eosin

Pathologic confirmation of breast cancer was conducted on paraffin-embedded tissue sections of 5 mm thickness stained with hematoxylin and eosin (H&E) and reviewed by a pathologist (R.C. Dash) blinded to group assignment.

Immunohistochemistry

Histologically confirmed breast cancer sections (obtained at week 9) were treated with 5% hydrogen peroxide in methanol, blocked with 10% normal bovine serum, and stained using specific antibodies. Specifically, to evaluate tumor microvessel/vasculature (endothelial cells), sections were incubated for 1 hour with rat anti-mouse CD-31 antibody (Dako; M0823) at a dilution of 1:30. The secondary antibody was biotinylated horse anti-mouse immunoglobulin G (IgG) from Vector (BA2020), used at 1:200 for 30 minutes. The detection was facilitated by the ready-to-use (RTU) ABC Elite Staining Kit from Vector (PK7100) for 30 minutes with 3,3'-diaminobenzidine (DAB) used as the chromogen from Dako (K3468) for 5 minutes (producing a brown color where antibody binding occurs). For all remaining antibodies, the secondary antibody was biotinylated goat anti-rabbit from Vector (BA1000) and used at a dilution of 1:200 for 30 minutes. The chromogen kit used was the same for all antibodies. The hypoxia marker hypoxia-inducible factor-1 α (HIF-1 α) was assessed using a rabbit polyclonal antibody (Novus; NB100-479) at a dilution of 1:400 for 45 minutes. GRP78, a major endoplasmic reticulum chaperone that is induced in response to cellular stress, was assessed using rabbit monoclonal antibody (Epitomics; 3158-1) at 1:1,000 for 30 minutes.

To evaluate tumor cell proliferation, sections were fixed with 4% paraformaldehyde, permeabilized with 0.5% saponin, and incubated overnight with rabbit monoclonal antibody against Ki-67 (LabVision; RM-9106-S) at a dilution of 1:300. Finally, to evaluate apoptosis, slides were stained with anticaspase-3 antibody (Cell Signaling Technology, Inc.), diluted at 1:200. All washes and antibody dilutions were conducted with 0.5% saponin in PBS. For the purpose of image presentation, pictures were taken using a Leica DMI6000CS inverted confocal microscope and Leica LAS AF 2.0 software. All images were captured at \times 5 magnification in 16-bit monochrome signal depth.

The nuclear counterstain permitted ROI contour lines to be constructed, permitting necrotic regions to be excluded on the basis of the absence of tumor cell nuclei. MVD was calculated for each section by overlaying a fixed grid on the CD-31 image (Adobe Photoshop CS2; Adobe Systems, Inc.). Individual CD-31-positive vessels were manually counted in every other visible field to determine a mean value for the section. All other immunostains were analyzed using ImageJ software (NIH, Bethesda, MD; <http://rsb.info.nih.gov/ij/>).

RNA amplification, labeling, and arrays

RNA was first converted to cDNA through a reverse transcription reaction with biotinylated primers. Next, biotinylated cDNA was annealed to assay oligonucleotides (oligos), and bound to streptavidin-conjugated paramagnetic particles (SA-PMP). After the oligo hybridization, mismatched and nonhybridized oligos were washed away, with subsequent extension and ligation of hybridized oligos. These products form a synthetic template that was

transferred to a PCR containing a fluorescently labeled primer. The labeled PCR product strand was isolated and the fluorescent products were hybridized to a whole-genome expression BeadChip. The BeadChip was washed and imaged on the iScan System or BeadArray Reader.

Microarray data preprocessing and analysis

Expression estimates were assessed using the Illumina Whole-Genome DASL Gene Expression Assay. Illumina BeadChips were obtained from the following preprocessing algorithm applied to all samples. Taking the raw bead averages from the array, data were processed by: (i) cubic-spline normalization, (ii) background subtraction, (iii) negative values were linearly truncated to be less than 2, and \log_2 transformed, and (iv) undetected transcripts were removed from the dataset, resulting in expression estimates for 20,793 features annotated to a total of 14,382 genes. Global patterns of gene expression were evaluated (with the top 10% of genes by coefficient of variation) by principal component analysis (PCA) and hierarchical clustering algorithms using the average linkage of the Pearson correlation coefficient.

Statistical analysis

Baseline medical and demographic characteristics of each group are summarized using descriptive statistics (mean/SD and frequencies) and compared. All between group differences with $P < 0.10$ were included as covariates in the change score analyses (only tumor met this criteria; the distribution of all other baseline characteristics were similar between study arms; $P > 0.20$). ANOVA was used for comparisons that involve normally distributed data. Nonparametric tests such as the Kruskal–Wallis test was used for continuous, non-normal data. Exact χ^2 tests were used to compare groups with respect to categorical variables.

The repeated measures data were fitted using linear mixed effects models and corrected for skewness where appropriate. For each outcome, the optimal variance–covariance structure for repeated measures among (i) compound symmetry, (ii) independent, and (iii) auto regressive correlation was selected. Optimal was defined as the variance–covariance structure that minimized Akaike Information Criteria (AIC) in the full model. Starting from a full model of treatment interaction with quadratic effect of time, reduced models were considered until a statistically significant effect was discernible (likelihood ratio test, $P < 0.05$). Time, group, and interaction effects were tested in the fitted models. All repeated measures analyses were conducted under the intention-to-treat (ITT) principle. The ITT analysis included all randomized participants in their randomly assigned group. Given the exploratory nature of this study, statistical analyses were not adjusted for multiple comparisons.

Differences in gene expression between study groups were evaluated using a Student *t* test. Pathway-level associations were made to gene sets derived from annotations to the Illumina platform for Gene Ontology (GO) and Kyoto Encyclopedia of Genes and Genomes (KEGG); inferences

were conducted using the robust resampling-based process, SAFE (47). Nominal thresholds are used in reporting *P* values to account for multiple testing. Specifically, the Benjamini–Hochberg step-up procedure was used to estimate the false discovery rate (FDR) from each gene- and pathway-level analysis. In brief, the Benjamini–Hochberg method controls the FDR in multiple hypotheses testing to correct for multiple comparisons.

Results

Details about response rates, profiles of the participants, and exercise adherence rates have been reported previously (40). Participant recruitment took place between March 2007 and June 2010. The groups were balanced at baseline (Table 1). One patient was lost to follow-up due to the development of deep vein thrombus and pulmonary embolism following randomization. Overall, adherence in the AC+AET group was 82% (296 attended/360 prescribed; range, 0%–100%). Overall, compliance to the planned exercise prescription was 66% (194 complied sessions/

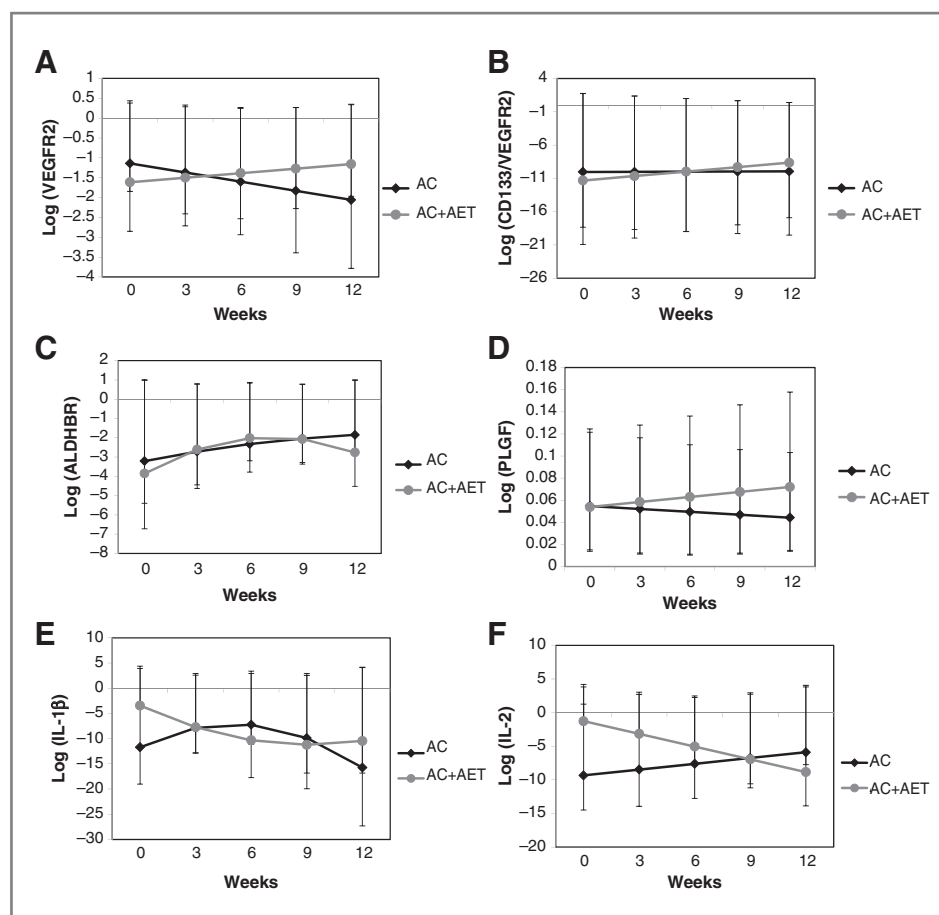
Table 1. Patient characteristics

Characteristic	AC (n = 10)	AC + AET (n = 10)
Age, y	46 ± 11	51 ± 6
Weight, kg	78 ± 25	78 ± 13
BMI, kg/m ²	28 ± 9	29 ± 5
Primary tumor size, no. of women (%)		
T1, ≤2 cm	3 (30)	—
T2, 2–5 cm	6 (60)	5 (50)
T3, >5 cm	1 (10)	5 (50)
Nodal status, no. of women (%)		
N0	4 (40)	5 (50)
N1	5 (50)	4 (40)
N2	1 (10)	1 (10)
Tumor histology, no. of women (%)		
Ductal	9 (90)	8 (80)
Lobular	1 (10)	2 (20)
Positive estrogen receptor or progesterone receptor status, no. of women (%)	4 (40)	5 (50)
HER2/neu status, no. of women (%)		
Positive	1 (10)	3 (30)
Negative	9 (90)	7 (70)
Concomitant comorbid disease, no. of women (%)		
Hypertension	4 (40)	1 (10)
Hyperlipidemia	3 (30)	1 (10)
Other (e.g., osteoarthritis, type II diabetes, etc.)	2 (20)	4 (40)

NOTE: Data presented as mean ± SD. All comparisons, $P > 0.10$ (tumor size, $P = 0.06$).

Abbreviation: BMI, body mass index.

Figure 4. Effect of AET conducted during concurrent neoadjuvant anthracycline and cyclophosphamide therapy (AC+AET) compared with neoadjuvant anthracycline and cyclophosphamide therapy alone (AC) on serial changes in cell surface expression markers of CEPs and selected circulating CAFs: (A) VEGFR-2, (B) CD-133/VEGFR-2, (C) ALDH^{br} cells, (D) soluble PLGF, (E) IL-1 β , and (F) IL-2. Values represent patient-averaged fitted model results, least squares means with confidence limits ($n = 6-8$ /group/time point; all $P < 0.05$ for group by time interaction, except ALDH^{br} cells).



296 attended). As a result, 34% of planned exercise sessions required dose modification. Major reasons for exercise dose modifications were nausea, tiredness/fatigue, and not feeling well. No serious adverse events were observed during AET sessions (40).

Changes in exercise capacity and endothelial function

$VO_{2\text{ peak}}$ increased from 19.5 ± 7.6 to 22.1 ± 7.0 $\text{mL}\cdot\text{kg}^{-1}\cdot\text{min}^{-1}$ ($P = 0.04$) in the AC+AET group, whereas it decreased from 17.5 ± 4.8 to 16.0 ± 4.0 $\text{mL}\cdot\text{kg}^{-1}\cdot\text{min}^{-1}$ ($P = 0.04$) in the AC group, resulting in a between group difference of more than 4.1 $\text{mL}\cdot\text{kg}^{-1}\cdot\text{min}^{-1}$ that favored the AC+AET group ($P < 0.01$), as reported previously (40). Endothelial-dependent BA-FMD, expressed as percentage change in brachial artery diameter, increased in both groups but to a greater extent in the AC + AET group [5.7 ± 1.8 to 6.4 ± 1.3 ($P = 0.07$)] compared with the AC group [5.2 ± 1.7 to 5.7 ± 2.7 ($P = 0.27$)]. The between group difference was not significant ($P = 0.26$).

Changes in circulating endothelial progenitor cells

Significant temporal time \times group interaction effects were observed for the CEP surface markers of VEGFR-2 and CD-133⁺-VEGFR-2⁺. Specifically, for both markers, there was a serial significant linear increase from baseline to week

12 in the AC+AET group compared with a serial significant linear decrease in the AC group ($P < 0.05$; Fig. 4A and B). Finally, serial linear increases were observed for ALDH in both groups, although this effect was attenuated in the AC+AET group from weeks 6 to 12 ($P > 0.05$; Fig. 4C).

Changes in plasma cytokines and angiogenic factors

Of the 19 CAFs, significant temporal time \times group interaction effects were observed for three CAFs. Specifically, a serial linear increase from baseline to week 12 was observed in the AC+AET group compared with serial linear decrease in the AC group for the proangiogenic factor placenta growth factor (PLGF; $P = 0.04$; Fig. 4D). For interleukin (IL)-1 β , a cytokine produced by activated macrophages and an important mediator of the inflammatory response, a monotonic (nonlinear) response was observed with IL-1 β declining in both groups from baseline to week 12. Specifically, in the AC+AET group, a serial decline was observed from weeks 0 to 6 followed by a plateau in weeks 9 to 12; in the AC group, there was an initial increase in IL-1 β in weeks 0 to 6, followed by a steady decline in weeks 9 to 12 ($P < 0.01$; Fig. 4E). Finally, a serial linear decrease from baseline to week 12 was observed in the AC+AET group compared with serial linear increase in the AC group for IL-2, a soluble cytokine and mediator of

immunity ($P = 0.02$; Fig. 4F). Of note, serial linear increases were observed for IL-8, a proangiogenic chemokine, in both groups although levels were consistently higher in the AC+AET group ($P < 0.05$ for both time and group effects; data not shown). There were no differences for any other CAFs (data not shown).

Changes in tumor blood flow/perfusion

^{15}O -labeled water PET scans were conducted at baseline and week 9 to assess tumor blood flow, using a ratio of PET activity in the tumor to activity in normal breast tissue. Unfortunately, due to technical reasons (e.g., machine malfunction, scheduling, etc.) pre-post PET scans were only available for 5 patients in the AC+AET and 2 patients in AC group (data not reported). The tumor to normal tissue ratio showed a decrease in the AC+AET group (mean reduction 38%; data not shown).

Effects on intratumoral neoplastic phenotype

Tumor biopsy samples were obtained at week 9 (i.e., third cycle of AC) in both groups. Because of pathologic complete response rates to AC therapy as well as degraded tissue, samples were only available on 5 patients per group. Histologic analysis of primary tumor tissue specimens indicated no differences in CD-31, HIF-1, GRP78 or proliferation and apoptosis ($P > 0.05$; data not shown).

Effects on tumor gene expression

Whole-genome microarray tumor analysis revealed three downregulated (*PAK4*, *FYB*, and *TNFRSF10D*) and four upregulated (*KREMEN1*, *LOC402057*, *SERPINA3*, and *NDUFS8*) transcripts in the AC+AET group compared with the AC group ($P < 0.05$; FDR at $<20\%$; Table 2). Interestingly, *PAK4*, *FYB*, and *TNFRSF10D* transcripts function in NF- κ B signaling, inflammation, and cell migration, whereas *KREMEN1*, *LOC402057*, *SERPINA3*, and *NDUFS8* have critical roles in maintaining oxidative phosphorylation, ribosome biogenesis, and inhibiting pathway signaling supporting inflammation and Wnt/ β -catenin activity. Subsequent pathway analysis revealed significant differential

modulation of 57 pathways (all $P < 0.01$), including many that converge on NF- κ B (Fig. 5).

Discussion

The purpose of this pilot study was to explore the effects of AET on several relevant host-related factors that could potentially modulate the antitumor properties of chemotherapy, as well as explore whether modulation of host-related factors altered tumor tissue markers in patients with breast cancer receiving neoadjuvant chemotherapy. These initial pilot results suggest that AET during concurrent chemotherapy causes provascular (physiologic) adaptations in host physiology and circulating factors that occur in conjunction with alteration in tumor gene expression, compared with chemotherapy alone. Findings of this exploratory study suggest that the effects of AET during adjuvant therapy may extend beyond improving symptom-control endpoints to also modulate host-related pathways that could, in theory, alter tumor phenotype and/or therapeutic response. Nevertheless, it is important to state that our data are by no means definitive and the clinical or biologic importance of our findings remains to be determined. Also, caution is required while interpreting our findings given the highly exploratory nature of this pilot study and small sample size.

In cardiovascular medicine, it is well established that AET exerts a multitude of favorable (physiologic) vascular (i.e., endothelial function) adaptations; these adaptations have been observed in several clinical populations including patients with overt coronary artery disease (17, 18), type II diabetes (19, 20), and chronic heart failure (21). These effects are postulated to contribute, in part, to the plethora of AET-associated cardiovascular health benefits (48). AET-induced increased NO biosynthesis is a major mediator of the favorable cardiovascular adaptations (48, 49). Specifically, in response to AET-induced repeated exposure of the vasculature to shear stress, VEGF is secreted into the systemic circulation leading to biosynthesis of NO through VEGFR-2 AKT-dependent endothelial NO synthase (eNOS) phosphorylation (50). In tumor biology research, both NO and

Table 2. The top over-represented transcripts in tumor between AC and AC+EX groups at 12 weeks^a

Transcripts	SAM ranking	Unigene or genome database name
Downregulated		
<i>FYB</i>	1	FYN-binding protein
<i>PAK4</i>	2	p21 protein (Cdc42/Rac)-activated kinase 4
<i>TNFRSF10D</i>	3	TNF receptor superfamily, member 10d, decoy with truncated death domain
Upregulated		
<i>KREMEN1</i>	1	Kringle-containing transmembrane protein 1
<i>LOC402057</i>	2	FROM EA: similar to 40S ribosomal protein S17 (LOC402057), mRNA.
<i>SERPINA3</i>	3	Serpin peptidase inhibitor, clade A (α -1 antiproteinase, antitrypsin), member 3
<i>NDUFS8</i>	4	NADH dehydrogenase (ubiquinone) Fe-S protein 8, 23kDa (NADH-coenzyme Q reductase)

^aDownregulated pathways are those where gene-expression is lower in the AC+AET group compared with AC, whereas upregulated transcripts are those where gene-expression is higher in the AC+AET group compared with AC.

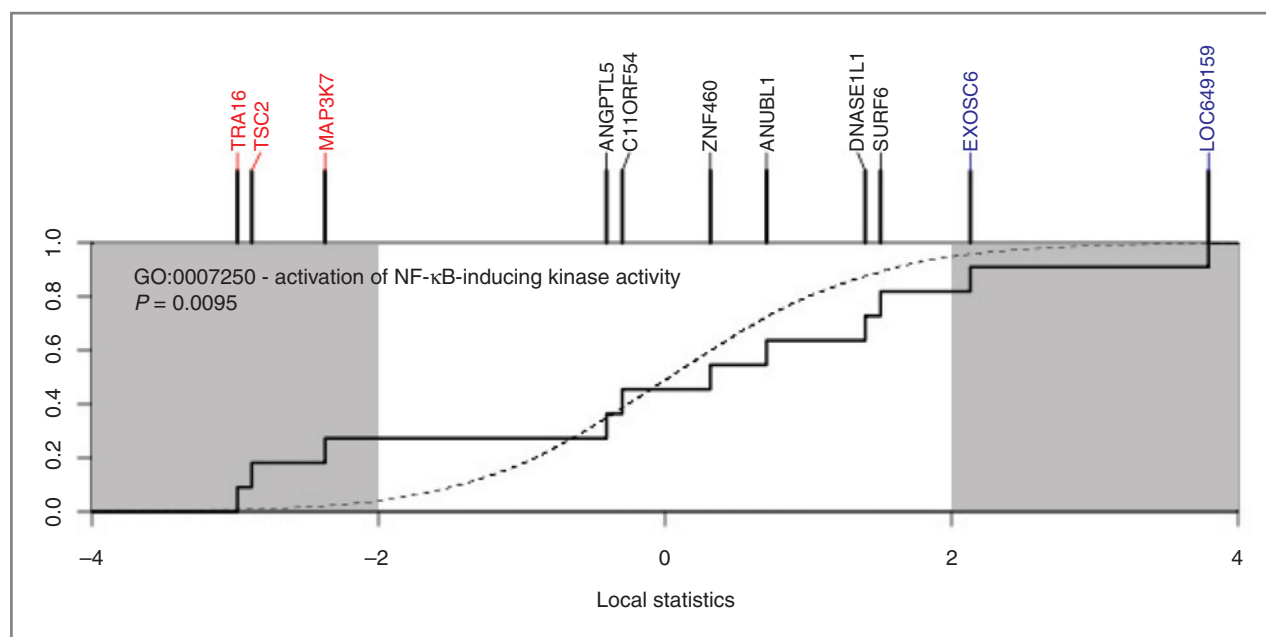


Figure 5. SAFE plot of pathway-level differential gene expression for the effect of AET conducted during concurrent neoadjuvant anthracycline and cyclophosphamide (AC+AET) therapy compared with neoadjuvant anthracycline and cyclophosphamide therapy alone (AC). Genes annotated to the NF- κ B pathway show significant downregulation (red) and upregulation (blue) in patients undergoing aerobic training.

eNOS have received considerable attention across a wide variety of cancer-related events including tumor apoptosis, cell cycle, initiation/progression, and metastasis (51, 52). Not surprisingly, given that it is a potent regulator of regional blood flow, NO has been investigated in tumor angiogenesis as well as modulation of chemosensitivity (53). On this basis, investigators have examined the efficacy of strategies that may augment NO-bioavailability, as well as other proangiogenic factors, to improve therapeutic sensitization including diethylamine NO (54), hyperbaric oxygen (55–57), hyperthermia (58–61), and human recombinant erythropoietin (62–66) with mixed results. Further research on the modulating effects of AET-induced increases in systemic NO bioavailability and therapeutic sensitization is warranted.

To examine systemic regulators of NO biosynthesis, we investigated the dynamic (serial) change in circulating CAFs. Although VEGF is a potent activator of eNOS in endothelial cells, no changes in circulating VEGF levels were detected across time in either group (data not shown). Moreover, no differences were observed for granulocyte macrophage colony-stimulating factor (GM-CSF), another known inducer of NO (data not shown). Dynamic changes were, however, observed in three circulating CAFs (i.e., PLGF, IL-1 β , and IL-2); in general, these factors decreased in the AET group compared with serial increases in the AC group. Host-derived CAFs can contribute to a "tumorigenic" host milieu that facilitates all steps in the metastatic cascade as well as altering the response to antitumor therapy (67, 68). In addition, treatment with certain anticancer therapies cause distinct changes in circulating CAFs (e.g., VEGF, PLGF, and sVEGFR-2) that can promote a "protumorigenic" host

environment (67, 69, 70). Strategies that can therefore "neutralize" host and/or therapy-induced release of CAFs may be a promising approach to improve clinical outcomes in patients with solid tumors (67). Findings of this study, together with prior work (11, 71, 72), provide initial evidence that chronic (repeated) AET may modulate circulating concentrations of select CAFs. Whether AET also alters CAF concentrations in the tumor microenvironment to directly influence tumor angiogenesis or tumor cell behavior has not been investigated.

NO also activates the release and mobilization of CEPs and other bone marrow-derived cells (BMDC) via matrix metalloproteinase-9 (MMP-9)-dependent mechanisms (26). Consistent with prior work in cardiac populations (22, 37, 38), we observed that AET significantly increased the number of CEPs, identified on the basis of validated cell surface expression markers (i.e., CD-133 and VEGFR-2). Interestingly, while AET was associated with robust effects on the CEP cell surface markers CD-133 and VEGFR-2, there were no effects for the surface marker ALDH. A potential explanation for these discrepant findings is that ALDH has been postulated to be a marker for all progenitor cell types (73), and thus may not be specific to cells of an endothelial lineage (i.e., CD-133 and VEGFR-2) which, in turn, suggests that the effects of AET may be specific to progenitors of this lineage.

In response to a number of gene signals, CEPs enter the peripheral circulation, migrate to sites of angiogenesis, and incorporate into growing vessels (26). In the setting of cardiovascular disease, AET-induced increases in CEPs enhance physiologic angiogenesis and augment endothelial function leading to enhanced recovery in models of

myocardial ischemia (74). Interestingly, our initial pre-clinical work indicates that exercise (voluntary wheel running) may exert similar effects in solid tumors. Specifically, we observed that exercise causes enhanced intratumoral perfusion/vascularization leading to decreased hypoxia (i.e., a more "normalized" tumor microenvironment) in mouse models of breast and prostate cancer (11, 39). We speculate that exercise-induced increases in CEPs may contribute to this phenomenon, although no study to date has investigated this question. AET-induced enhanced NO-biosynthesis and mobilization of CEPs may also have implications for the therapeutic index of certain anticancer strategies. Intratumoral hypoxia is a major contributor to therapeutic resistance across a number of antitumor strategies, including chemotherapy (75, 76). As such, AET-induced reductions in intratumoral hypoxia, possibly via modulation of systemic (host-related) CAFs, may decrease therapeutic resistance by augmenting tumor blood perfusion, leading to increased chemo- or radiosensitization. In support of this notion, our group recently observed that the combination of exercise (voluntary wheel running) and chemotherapy (cyclophosphamide) was associated with significantly prolonged tumor growth delay compared with chemotherapy alone in a mouse model of murine breast cancer (77).

Although we speculate that AET-induced increases in CEPs may enhance therapeutic efficacy the opposite, in theory, could also be plausible. CEPs, critical regulators of tumor angiogenesis and the establishment of "pre-metastatic" niches (78), contribute to the repopulation of tumor cells to collectively facilitate invasion and metastasis as well as compromise therapeutic efficacy (79). As such, selective inhibition of CEPs has been proposed as a potential therapeutic strategy against solid tumors (67). Thus, findings of the present study showing AET-induced serial increases in CEPs is clearly in direct contrast to this therapeutic goal and instead suggest that AET could facilitate the acquisition of an invasive tumor phenotype or acceleration of metastasis. Such equipoise highlights the urgent need for future studies to carefully dissect the complex and multifaceted effects of AET on the host-tumor interaction and response to therapy.

Our study was neither designed nor adequately powered to investigate whether the addition of AET to conventional neoadjuvant chemotherapy improved clinical response compared with chemotherapy only. With a view toward future studies, we did, however, explore whether AET modulated several correlative biomarkers of tumor response to chemotherapy including tumor blood flow (with PET) as well as markers of the tumor neoplastic phenotype. Specifically, tumor blood flow decreased, on average, 38% from baseline to week 9 in the AC+AET group. However, due to repeated technical difficulties (e.g., machine malfunction, scheduling) pre-post imaging were only available for a minority of patients in both groups. Similarly, due to AC-induced pathologic complete response rates and degraded tissue a small number of tumor biopsies were also obtained. Not surprisingly, there were no between-group differences on any markers of the tumor phenotype

relating to MVD (CD-31), hypoxia (HIF-1 α), or autophagy (GRP78) as well as proliferation or apoptosis. Consequently, the effects of AET on tumor blood flow/physiology and markers of the neoplastic phenotype remains inconclusive requiring further study.

Finally, we used whole-genome tumor microarray to explore other pathways that may be modulated by AET. Interestingly, transcripts functioning in NF- κ B signaling and inflammation were downregulated in the AET+AC group compared with AC alone. Subsequent pathway analysis revealed significant modulation of 57 pathways including many that also signal through NF- κ B. NF- κ B is a central mediator of tumor inflammation, angiogenesis, and invasion and is constitutively overexpressed in a variety of solid tumors. Of relevance, in a recent "window of opportunity" phase II trial, Heymach and colleagues (80) found that compared with a usual diet, low-fat diet reduced circulating levels of specific CAFs, all of which are regulated by NF- κ B in men with localized prostate cancer. NF- κ B plays a critical role in regulating host-response to perturbations in energy balance, particularly high-fat diet, as well as the effects of AET on the inflammatory response (81, 82).

In conclusion, the application of AET to prevent and/or off-set disease and/or treatment-related toxicities to optimize symptom control and recovery is becoming increasingly accepted in the oncology setting. More recently, there has also been growing interest to elucidate the systemic and molecular mechanistic properties of AET to modulate tumor progression/metastasis as well as therapeutic response. Preoperative window of opportunity studies, with or without concurrent anticancer therapy, provide an ideal setting to conduct "proof-of-concept" trials investigating the effects of AET on tumor biology in conjunction with blood-based and imaging correlative biomarkers to inform "smart" definitive phase II/III trials. However, in the neoadjuvant setting, effects of AET on study endpoints of interest may be difficult to interpret and/or show beyond those induced by cytotoxic therapy.

To this end, findings from the present study provide the first evidence that supervised AET interventions are feasible in the neoadjuvant breast cancer setting. Furthermore, while the biologic and clinical implications remain to be determined, this work also provides initial evidence that AET can modulate several host- and tumor-related pathways (beyond standard chemotherapy) that may, in turn, have implications for cancer-related events and therapeutic response. Overall, we hope that results of this pilot study will inform and stimulate the development of future studies in this area of research.

Disclosure of Potential Conflicts of Interest

G. Broadwater is a consultant/advisory board member of Public Library of Science. No potential conflicts of interest were disclosed by the other authors.

Authors' Contributions

Conception and design: L.W. Jones, W.T. Barry, L.G. Wilke, K.L. Blackwell
Development of methodology: L.W. Jones, D.R. Fels, T.J. Povsic, J.D. Allen

Acquisition of data (provided animals, acquired and managed patients, provided facilities, etc.): L.W. Jones, D.R. Fels, L.G. Wilke, E. Masko, T.J. Povsic, P.K. Marcom, K.L. Blackwell, G. Kimmick, J.D. Allen

Analysis and interpretation of data (e.g., statistical analysis, biostatistics, computational analysis): L.W. Jones, G. Broadwater, W.T. Barry, E. Masko, R.C. Dash, T.J. Povsic, M.W. Dewhirst, J.D. Allen

Writing, review, and/or revision of the manuscript: L.W. Jones, D.R. Fels, G. Broadwater, W.T. Barry, E. Masko, P.S. Douglas, T.J. Povsic, J. Peppercorn, P.K. Marcom, K.L. Blackwell, G. Kimmick, M.W. Dewhirst, J.D. Allen

Study supervision: L.W. Jones, M. West, K.L. Blackwell, J.D. Allen

Grant Support

This study was supported by the United States Department of Defense Breast Cancer Research Program of the Office of the Congressionally Directed Medical Research Programs—Ideas Award (to L.W. Jones). M.W. Dewhirst is supported by NIH CA40355.

The costs of publication of this article were defrayed in part by the payment of page charges. This article must therefore be hereby marked *advertisement* in accordance with 18 U.S.C. Section 1734 solely to indicate this fact.

Received October 10, 2012; revised May 20, 2013; accepted June 13, 2013; published OnlineFirst July 10, 2013.

References

- Mishra SI, Scherer RW, Geigle PM, Berlanstein DR, Topaloglu O, Gotay CC, et al. Exercise interventions on health-related quality of life for cancer survivors. *Cochrane Database Syst Rev* 2012;8:CD007566.
- Mishra SI, Scherer RW, Snyder C, Geigle PM, Berlanstein DR, Topaloglu O. Exercise interventions on health-related quality of life for people with cancer during active treatment. *Cochrane Database Syst Rev* 2012;8:CD008465.
- McNeely ML, Campbell KL, Rowe BH, Klassen TP, Mackey JR, Courneya KS. Effects of exercise on breast cancer patients and survivors: a systematic review and meta-analysis. *CMAJ* 2006;175:34–41.
- Schmitz KH, Courneya KS, Matthews C, Demark-Wahnefried W, Galvao DA, Pinto BM, et al. American College of Sports Medicine roundtable on exercise guidelines for cancer survivors. *Med Sci Sports Exerc* 2010;42:1409–26.
- Speck RM, Courneya KS, Masse LC, Duval S, Schmitz KH. An update of controlled physical activity trials in cancer survivors: a systematic review and meta-analysis. *J Cancer Surviv* 2010;4:87–100.
- Rock CL, Doyle C, Demark-Wahnefried W, Meyerhardt J, Courneya KS, Schwartz AL, et al. Nutrition and physical activity guidelines for cancer survivors. *CA Cancer J Clin* 2012;62:242–74.
- Hayes SC, Spence RR, Galvao DA, Newton RU. Australian association for exercise and sport science position stand: optimising cancer outcomes through exercise. *J Sci Med Sport* 2009;12:428–34.
- van den Berg JP, Velthuis MJ, Gijzen BC, Lindeman E, van der Pol MA, Hillen HF. Guideline cancer rehabilitation. *Ned Tijdschr Geneesk* 2011;155:A4104.
- Jones LW, Eves ND, Haykowsky M, Freedland SJ, Mackey JR. Exercise intolerance in cancer and the role of exercise therapy to reverse dysfunction. *Lancet Oncol* 2009;10:598–605.
- Pedersen BK, Febbraio MA. Muscles, exercise and obesity: skeletal muscle as a secretory organ. *Nat Rev Endocrinol* 2012;8:457–65.
- Jones LW, Antonelli J, Masko EM, Broadwater G, Lascola CD, Fels D, et al. Exercise modulation of the host-tumor interaction in an orthotopic model of murine prostate cancer. *J Appl Physiol* 2012;113:263–72.
- Taghian AG, Abi-Raad R, Assaad SI, Casty A, Ancukiewicz M, Yeh E, et al. Paclitaxel decreases the interstitial fluid pressure and improves oxygenation in breast cancers in patients treated with neoadjuvant chemotherapy: clinical implications. *J Clin Oncol* 2005;23:1951–61.
- Hockel M, Schlenger K, Knoop C, Vaupel P. Oxygenation of carcinomas of the uterine cervix: evaluation by computerized O₂ tension measurements. *Cancer Res* 1991;51:6098–102.
- Moon EJ, Brizel DM, Chi JT, Dewhirst MW. The potential role of intrinsic hypoxia markers as prognostic variables in cancer. *Antioxid Redox Signal* 2007;9:1237–94.
- Brizel DM, Scully SP, Harrelson JM, Layfield LJ, Dodge RK, Charles HC, et al. Radiation therapy and hyperthermia improve the oxygenation of human soft tissue sarcomas. *Cancer Res* 1996;56:5347–50.
- Bos R, van der Groep P, Greijer AE, Shvarts A, Meijer S, Pinedo HM, et al. Levels of hypoxia-inducible factor-1alpha independently predict prognosis in patients with lymph node negative breast carcinoma. *Cancer* 2003;97:1573–81.
- Edwards DG, Schofield RS, Lennon SL, Pierce GL, Nichols WW, Braith RW. Effect of exercise training on endothelial function in men with coronary artery disease. *Am J Cardiol* 2004;93:617–20.
- Hambrecht R, Wolf A, Gielen S, Linke A, Hofer J, Erbs S, et al. Effect of exercise on coronary endothelial function in patients with coronary artery disease. *N Engl J Med* 2000;342:454–60.
- Allen JD, Geaghan JP, Greenway F, Welsch MA. Time course of improved flow-mediated dilation after short-term exercise training. *Med Sci Sports Exerc* 2003;35:847–53.
- Allen JD, Welsch M, Aucoin N, Wood R, Lee M, LeBlanc KE. Forearm vasoreactivity in type 1 diabetic subjects. *Can J Appl Physiol* 2001;26:34–43.
- Hambrecht R, Fiehn E, Weigl C, Gielen S, Hamann C, Kaiser R, et al. Regular physical exercise corrects endothelial dysfunction and improves exercise capacity in patients with chronic heart failure. *Circulation* 1998;98:2709–15.
- Laufs U, Urhausen A, Werner N, Scharhag J, Heitz A, Kissner G, et al. Running exercise of different duration and intensity: effect on endothelial progenitor cells in healthy subjects. *Eur J Cardiovasc Prev Rehabil* 2005;12:407–14.
- Kingwell BA. Nitric oxide-mediated metabolic regulation during exercise: effects of training in health and cardiovascular disease. *FASEB J* 2000;14:1685–96.
- Kingwell BA. Nitric oxide as a metabolic regulator during exercise: effects of training in health and disease. *Clin Exp Pharmacol Physiol* 2000;27:239–50.
- Kingwell BA, Jennings GL, Dart AM. Exercise and endothelial function. *Circulation* 2000;102:E179.
- Aicher A, Heeschen C, Mildner-Rihm C, Urbich C, Ihling C, Technau-Ihling K, et al. Essential role of endothelial nitric oxide synthase for mobilization of stem and progenitor cells. *Nat Med* 2003;9:1370–6.
- Asahara T, Murohara T, Sullivan A, Silver M, van der Zee R, Li T, et al. Isolation of putative progenitor endothelial cells for angiogenesis. *Science* 1997;275:964–7.
- Dimmeler S, Aicher A, Vasa M, Mildner-Rihm C, Adler K, Tiemann M, et al. HMG-CoA reductase inhibitors (statins) increase endothelial progenitor cells via the PI3-kinase/Akt pathway. *J Clin Invest* 2001;108:391–7.
- Jiang S, Walker L, Afentoulis M, Anderson DA, Jauron-Mills L, Corless CL, et al. Transplanted human bone marrow contributes to vascular endothelium. *Proc Natl Acad Sci U S A* 2004;101:16891–6.
- Kalka C, Masuda H, Takahashi T, Kalka-Moll WM, Silver M, Kearney M, et al. Transplantation of *ex vivo* expanded endothelial progenitor cells for therapeutic neovascularization. *Proc Natl Acad Sci U S A* 2000;97:3422–7.
- Llevadot J, Murasawa S, Kureishi Y, Uchida S, Masuda H, Kawamoto A, et al. HMG-CoA reductase inhibitor mobilizes bone marrow-derived endothelial progenitor cells. *J Clin Invest* 2001;108:399–405.
- Murohara T, Ikeda H, Duan J, Shintani S, Sasaki K, Eguchi H, et al. Transplanted cord blood-derived endothelial precursor cells augment postnatal neovascularization. *J Clin Invest* 2000;105:1527–36.
- Takahashi T, Kalka C, Masuda H, Chen D, Silver M, Kearney M, et al. Ischemia- and cytokine-induced mobilization of bone marrow-derived

- endothelial progenitor cells for neovascularization. *Nat Med* 1999;5:434–8.
34. Urbich C, Heeschen C, Aicher A, Sasaki K, Bruhl T, Farhadi MR, et al. Cathepsin L is required for endothelial progenitor cell-induced neovascularization. *Nat Med* 2005;11:206–13.
 35. Shaked Y, Henke E, Roodhart JM, Mancuso P, Langenberg MH, Colleoni M, et al. Rapid chemotherapy-induced acute endothelial progenitor cell mobilization: implications for antiangiogenic drugs as chemosensitizing agents. *Cancer Cell* 2008;14:263–73.
 36. Shaked Y, Ciarrocchi A, Franco M, Lee CR, Man S, Cheung AM, et al. Therapy-induced acute recruitment of circulating endothelial progenitor cells to tumors. *Science* 2006;313:1785–7.
 37. Schlager O, Giurgea A, Schuhfried O, Seidinger D, Hammer A, Groger M, et al. Exercise training increases endothelial progenitor cells and decreases asymmetric dimethylarginine in peripheral arterial disease: a randomized controlled trial. *Atherosclerosis* 2011;217:240–8.
 38. Steiner S, Niessner A, Ziegler S, Richter B, Seidinger D, Pleiner J, et al. Endurance training increases the number of endothelial progenitor cells in patients with cardiovascular risk and coronary artery disease. *Atherosclerosis* 2005;181:305–10.
 39. Jones LW, Viglianti BL, Tashjian JA, Kothadia SM, Keir ST, Freedland SJ, et al. Effect of aerobic exercise on tumor physiology in an animal model of human breast cancer. *J Appl Physiol* 2010;108:343–8.
 40. Hornsby WE, Douglas PS, West MJ, Kenjale AA, Lane AR, Schwitzer ER, et al. Safety and efficacy of aerobic training in operable breast cancer patients receiving neoadjuvant chemotherapy: a phase II randomized trial. *Acta Oncol*. In press.
 41. Say EA, Melamud A, Esserman DA, Povsic TJ, Chavala SH. Comparative analysis of circulating endothelial progenitor cells in age-related macular degeneration patients using automated rare cell analysis (ARCA) and fluorescence activated cell sorting (FACS). *PLoS ONE* 2013;8:e55079.
 42. Jones LW, Courneya KS, Mackey JR, Muss HB, Pituskin EN, Scott JM, et al. Cardiopulmonary function and age-related decline across the breast cancer survivorship continuum. *J Clin Oncol* 2012;30:2530–7.
 43. Duscha BD, Robbins JL, Jones WS, Kraus WE, Lye RJ, Sanders JM, et al. Angiogenesis in skeletal muscle precede improvements in peak oxygen uptake in peripheral artery disease patients. *Arterioscler Thromb Vasc Biol* 2011;31:2742–8.
 44. Welsch MA, Allen JD, Geaghan JP. Stability and reproducibility of brachial artery flow-mediated dilation. *Med Sci Sports Exerc* 2002;34:960–5.
 45. Povsic TJ, Zavodni KL, Vainorius E, Kherani JF, Goldschmidt-Clermont PJ, Peterson ED. Common endothelial progenitor cell assays identify discrete endothelial progenitor cell populations. *Am Heart J* 2009;157:335–44.
 46. Povsic TJ, Zavodni KL, Kelly FL, Zhu S, Goldschmidt-Clermont PJ, Dong C, et al. Circulating progenitor cells can be reliably identified on the basis of aldehyde dehydrogenase activity. *J Am Coll Cardiol* 2007;50:2243–8.
 47. Gatti DM, Barry WT, Nobel AB, Rusyn I, Wright FA. Heading down the wrong pathway: on the influence of correlation within gene sets. *BMC Genomics* 2010;11:574.
 48. Joyner MJ, Green DJ. Exercise protects the cardiovascular system: effects beyond traditional risk factors. *J Physiol* 2009;587(Pt 23):5551–8.
 49. Green DJ, Maiorana A, O'Driscoll G, Taylor R. Effect of exercise training on endothelium-derived nitric oxide function in humans. *J Physiol* 2004;561(Pt 1):1–25.
 50. Gielen S, Sandri M, Erbs S, Adams V. Exercise-induced modulation of endothelial nitric oxide production. *Curr Pharm Biotechnol* 2011;12:1375–84.
 51. Lim KH, Ancrile BB, Kashatus DF, Counter CM. Tumour maintenance is mediated by eNOS. *Nature* 2008;452:646–9.
 52. Ying L, Hofseth LJ. An emerging role for endothelial nitric oxide synthase in chronic inflammation and cancer. *Cancer Res* 2007;67:1407–10.
 53. Matthews NE, Adams MA, Maxwell LR, Gofton TE, Graham CH. Nitric oxide-mediated regulation of chemosensitivity in cancer cells. *J Natl Cancer Inst* 2001;93:1879–85.
 54. Shan SQ, Rosner GL, Braun RD, Hahn J, Pearce C, Dewhirst MW. Effects of diethylamine/nitric oxide on blood perfusion and oxygenation in the R3230Ac mammary carcinoma. *Br J Cancer* 1997;76:429–37.
 55. Annane D, Depondt J, Aubert P, Villart M, Gehanno P, Gajdos P, et al. Hyperbaric oxygen therapy for radionecrosis of the jaw: a randomized, placebo-controlled, double-blind trial from the ORN96 study group. *J Clin Oncol* 2004;22:4893–900.
 56. Bui QC, Lieber M, Withers HR, Corson K, van Rijnsoever M, Elsaleh H. The efficacy of hyperbaric oxygen therapy in the treatment of radiation-induced late side effects. *Int J Radiat Oncol Biol Phys* 2004;60:871–8.
 57. Kaanders JH, Bussink J, van der Kogel AJ. Clinical studies of hypoxia modification in radiotherapy. *Semin Radiat Oncol* 2004;14:233–40.
 58. Vujaskovic Z, Rosen EL, Blackwell KL, Jones EL, Brizel DM, Prosnitz LR, et al. Ultrasound guided pO₂ measurement of breast cancer reoxygenation after neoadjuvant chemotherapy and hyperthermia treatment. *Int J Hyperthermia* 2003;19:498–506.
 59. Zywiets F, Reeker W, Kochs E. Changes in tumor oxygenation during a combined treatment with fractionated irradiation and hyperthermia: an experimental study. *Int J Radiat Oncol Biol Phys* 1997;37:155–62.
 60. Jones EL, Prosnitz LR, Dewhirst MW, Marcom PK, Hardenbergh PH, Marks LB, et al. Thermochemoradiotherapy improves oxygenation in locally advanced breast cancer. *Clin Cancer Res* 2004;10:4287–93.
 61. Feldmann HJ, Molls M, Fuller J, Stuben G, Sack H. Changes in oxygenation patterns of locally advanced recurrent tumors under thermoradiotherapy. *Adv Exp Med Biol* 1994;345:479–83.
 62. Golab J, Olszewska D, Mroz P, Kozar K, Kaminski R, Jalili A, et al. Erythropoietin restores the antitumor effectiveness of photodynamic therapy in mice with chemotherapy-induced anemia. *Clin Cancer Res* 2002;8:1265–70.
 63. Henke M, Laszig R, Rube C, Schafer U, Haase KD, Schilcher B, et al. Erythropoietin to treat head and neck cancer patients with anaemia undergoing radiotherapy: randomised, double-blind, placebo-controlled trial. *Lancet* 2003;362:1255–60.
 64. Kotasek D, Steger G, Faught W, Underhill C, Poulsen E, Colowick AB, et al. Darbepoetin alfa administered every 3 weeks alleviates anaemia in patients with solid tumours receiving chemotherapy: results of a double-blind, placebo-controlled, randomised study. *Eur J Cancer* 2003;39:2026–34.
 65. Vansteenkiste J, Pirker R, Massuti B, Barata F, Font A, Fiegl M, et al. Double-blind, placebo-controlled, randomized phase III trial of darbepoetin alfa in lung cancer patients receiving chemotherapy. *J Natl Cancer Inst* 2002;94:1211–20.
 66. Blackwell KL, Kirkpatrick JP, Snyder SA, Broadwater G, Farrell F, Jolliffe L, et al. Human recombinant erythropoietin significantly improves tumor oxygenation independent of its effects on hemoglobin. *Cancer Res* 2003;63:6162–5.
 67. Kerbel RS, Ebos JM. Peering into the aftermath: the inhospitable host? *Nat Med* 2010;16:1084–5.
 68. Goodwin PJ, Meyerhardt JA, Hursting SD. Host factors and cancer outcome. *J Clin Oncol* 2010;28:4019–21.
 69. Hanrahan EO, Lin HY, Kim ES, Yan S, Du DZ, McKee KS, et al. Distinct patterns of cytokine and angiogenic factor modulation and markers of benefit for vandetanib and/or chemotherapy in patients with non-small-cell lung cancer. *J Clin Oncol* 2010;28:193–201.
 70. Kopetz S, Hoff PM, Morris JS, Wolff RA, Eng C, Glover KY, et al. Phase II trial of infusional fluorouracil, irinotecan, and bevacizumab for metastatic colorectal cancer: efficacy and circulating angiogenic biomarkers associated with therapeutic resistance. *J Clin Oncol* 2010;28:453–9.
 71. Fairey AS, Courneya KS, Field CJ, Bell GJ, Jones LW, Martin BS, et al. Effect of exercise training on C-reactive protein in postmenopausal breast cancer survivors: a randomized controlled trial. *Brain Behav Immun* 2005;19:381–8.

72. Jones LW, Eves ND, Peddle CJ, Courneya KS, Haykowsky M, Kumar V, et al. Effects of presurgical exercise training on systemic inflammatory markers among patients with malignant lung lesions. *Appl Physiol Nutr Metab* 2009;34:197–202.
73. Elsheikh E, Uzunel M, He Z, Holgersson J, Nowak G, Sumitran-Holgersson S. Only a specific subset of human peripheral-blood monocytes has endothelial-like functional capacity. *Blood* 2005;106:2347–55.
74. Laufs U, Werner N, Link A, Endres M, Wassmann S, Jurgens K, et al. Physical training increases endothelial progenitor cells, inhibits neointima formation, and enhances angiogenesis. *Circulation* 2004;109:220–6.
75. Dewhirst MW, Cao Y, Moeller B. Cycling hypoxia and free radicals regulate angiogenesis and radiotherapy response. *Nat Rev Cancer* 2008;8:425–37.
76. Jain RK. Normalizing tumor microenvironment to treat cancer: bench to bedside to biomarkers. *J Clin Oncol* 2013;31:2205–18.
77. Betof AS, Jones LW, Dewhirst MW. Exercise slows tumor progression and normalizes tumor vasculature in murine models of breast cancer (abstract). *Proceedings of the 104th Annual Meeting of the American Association for Cancer Research 2013*. 2013:Abstract nr 364.
78. Kaplan RN, Riba RD, Zacharoulis S, Bramley AH, Vincent L, Costa C, et al. VEGFR1-positive haematopoietic bone marrow progenitors initiate the pre-metastatic niche. *Nature* 2005;438:820–7.
79. Paez-Ribes M, Allen E, Hudock J, Takeda T, Okuyama H, Vinals F, et al. Antiangiogenic therapy elicits malignant progression of tumors to increased local invasion and distant metastasis. *Cancer Cell* 2009;15:220–31.
80. Heymach JV, Shackelford TJ, Tran HT, Yoo SY, Do KA, Wergin M, et al. Effect of low-fat diets on plasma levels of NF-kappaB-regulated inflammatory cytokines and angiogenic factors in men with prostate cancer. *Cancer Prev Res* 2011;4:1590–8.
81. Lima-Cabello E, Cuevas MJ, Garatachea N, Baldini M, Almar M, Gonzalez-Gallego J. Eccentric exercise induces nitric oxide synthase expression through nuclear factor-kappaB modulation in rat skeletal muscle. *J Appl Physiol* 2010;108:575–83.
82. Serra AJ, Santos MH, Bocalini DS, Antonio EL, Levy RF, Santos AA, et al. Exercise training inhibits inflammatory cytokines and more than prevents myocardial dysfunction in rats with sustained beta-adrenergic hyperactivity. *J Physiol* 2010;588(Pt 13):2431–42.